CHAPTER IV
ORGANIC-INORGANIC GREEN POROUS HYBRID COMPOSITE FOR GASSEPARATION

4.1 Abstract

The increasing of Earth's average temperature is one of the major problems that are caused by the emission of greenhouse gases (CO_2, CH_4). CO_2 is also considered as impurity gas in the natural gas, which mostly containing methane (CH_4). In this work, green porous hybrid composites were investigated for membrane separation application. The composites were prepared from non-toxic materials—polyvinyl alcohols (PVA) as a matrix, calcium carbonate ($CaCO_3$) was incorporated as a filler, and boric acid as a cross-linking agent—by using the freeze-drying method. The amounts of PVA and $CaCO_3$ were varied in order to obtain synergistic properties. Moreover, the densities of the composites were characterized by helium pycnometer. In addition, the N_2 adsorption/desorption isotherm (BET) and scanning electron microscopy (SEM) were used for the morphological study. The CO_2 and CH_4 permeability were determined by completing a single gas permeation experiment under room temperature and the pressure difference across samples of 10 psi. The composite showed better CH_4 permeability than that of CO_2 due to smaller molecular kinetic diameter traveling in the 3-D network pathways.

4.2 Introduction

Nowadays, the environmental issues are concerned because the rapidly increasing in the earth's average temperature is one of the major important that caused by the pollution of traditional plastic wastes release toxic gas and greenhouse gas (GHG) emissions. The emission of greenhouse gas includes carbon dioxide (CO_2) and methane (CH_4) into the atmosphere impacted on the global warming. Besides, CO_2 is an acidic gas, which can corrode the pipeline in the natural gas processing and reduce the energy content of natural gas (Li, *et al.*, 2010).

The preparation of materials which are environmentally friendly, non-toxic and or bio-sourced will be concerned due to environmental conservation by using the organic-inorganic hybrid composites. Moreover, most of all the mixtures are the combination of organic and inorganic in which the inorganic part acts as filler providing mechanical strength while the organic part as a matrix (Kickelbick, *et al.*, 2007). Polyvinyl alcohol (PVA) is an environmental synthetic polymer, non-toxic material, water soluble and biocompatible. For improving mechanical and thermal characteristics, polyvinyl alcohol-clay composite is interesting (Ali, *et al.*, 2012). In addition, calcium carbonate ($CaCO_3$) is the third most abundant material on earth Calcium carbonate has low cost and can be used to enhance the mechanical properties (Zheng, *et al.*, 2008 and Houmard, *et al.*, 2009).

In order to reduce CO_2 concentration, the separation of CO_2 from CH_4 can be also increase high-purity product and prevent the pipeline corrosion with membrane separation technique due to using- low-cost materials, low energy consumption, and safety environment (Sridhar, *et al.*, 2007). For gas separation, it can be divided into polymeric membrane, ceramic membrane and composite membrane (Abedini, *et al.*, 2010). Moreover, a membrane can be classified into porous and non-porous membranes. Porous membranes have advantages for high permeation of a permeate through the membrane but low selectivity (Zhang., 2010)

In this study, the preparation of green porous hybrid composite from polyvinyl alcohol (PVA) as a matrix combined with calcium carbonate ($CaCO_3$) used as a filler and cross-linking used boric acid, which are fabricated by using a

freeze-drying method in order to use for gas separation based on the porous composite properties has been investigated.

4.3 Experimental

4.3.1 Materials

Commercially available polyvinyl alcohol (PVA) with Mw = 108,000 g/mol and degree of hydrolysis of 99.7 was supplied from Polysciences. Calcium carbonate ($CaCO_3$) was from Sigma-Aldrich and boric acid, ($B(OH)_3$) was purchased from Merck. Distilled water was used throughout the experiment.

4.3.2 Measurements

The structure of samples after freeze-dried were tested the functional group of the composite by using a Nicolet Nexus 670 Fourier transform infrared spectrometer (FT-IR) with KBr pellet technique. Thermal analysis was detected by using Perkin Elmer Thermo gravimetric/Differential Thermal Analyzer (TG-DTA) under a nitrogen atmosphere with a flow rate 20ml/min and a heating rate of $10°Cmin^{-1}$. The surface morphology and microstructure of sample were observed by a scanning electron microscope (SEM) coating by gold under vacuum. The porous structures were tested by N_2 adsorption-desorption isotherm using a Quantachrome/Autosorb-1 at 77 K. and a He-pycnometer under room temperature.

4.3.3 Methodology

4.3.3.1 Preparation of Polyvinyl Alcohol/Calcium Carbonate Porous Hybrid Composite

Polyvinyl alcohol 0.3 g dissolved in 10 g of water (3, 5, 7% wt in distilled water) at the temperature in between 85-90°C 4h under continuous magnetic stirred until the completely dissolution of polymer then adding calcium carbonate by varies weight ratio of $PVA:CaCO_3$ (1:1,1:2,1:3,2:1,3:1) and stirred until homogenized mixture for 1 h.

The boric acid as a crosslinking agent was dropped into the solution (1M boric acid in water). The solution became high viscosity and placed it

into the mold. The hybrid composite solution was kept in refrigerator at 4°C followed by placing in freeze-dryer for 3 days.

4.3.3.2 Characterization Hybrid Porous PVA/CaCO₃ Composite

In this part, the samples after freeze-dried were tested the functional group of the composite by using Fourier transform infrared spectroscopy (FT-IR) from Thermo Nicolet. Thermal analysis was characterized by using Perkin Elmer Thermogravimetric/Differectial Thermal Analyzer (TG-DTA) under nitrogen atmosphere with heating rate 10°C/min. Porosity of porous $PVA/CaCO_3$ composite were measured by N_2 adsorption/desorption isotherm and Quantachrome, Ultrapycnometer1000 (He- Pycnometer) in order to obtain surface area, pore volume and. Surface morphology of porous materials suitable for application was studied from Scanning electron microscope (SEM).

4.3.3.3 Gas Separation Experiment

The single-component gas permeation experiments through the porous hybrid composite. For single gas study, the testing gas was flowed for 1 hour to get equilibrium state under room temperature. The CH_4 or CO_2 was fed to the upper side of stainless steel with pressure different across sample of about 10 psi. The area of a disc shape sample that contact with the gas was 0.53 cm². The flow rate was measured by using an ADM 1000 universal gas flow meter, Agilent technology. The permeance of the membrane was calculated using Eq. (1). A schematic diagram of a gas separation unit is shown in Figure 4.1.

$$\left(\frac{P}{\delta}\right)_i = \frac{Q_i \times 14.7 \times 10^6}{A \times (\Delta P) \times 76} \qquad (1)$$

Where; $\left(\frac{P}{\delta}\right)_i$ = permeance of gas 'i'(GPU)

[1 GPU = 1×10^{-6} (cm³ (STP))/(cm² s cmHg)]

P = permeability of gas 'i' (10^{-10} cm3 (STP) cm/ cm² s cmHg)

(1 Barrer = 10^{-10} cm3 (STP) cm/ cm² s cmHg = 7.5×10^{-18} m² s⁻¹ Pa⁻¹)

δ = thickness of membrane (μm)

Q_i = volumetric flow rate of gas 'i' (cm²/sec)

A = membrane area (cm²)

ΔP = pressure different between the feed side and permeating side (psi)

The ideal gas separation factor (Gas selectivity, $S_{A/B}$) for the component A and B is defined as the ratio of each component as shown in Eq. (2)
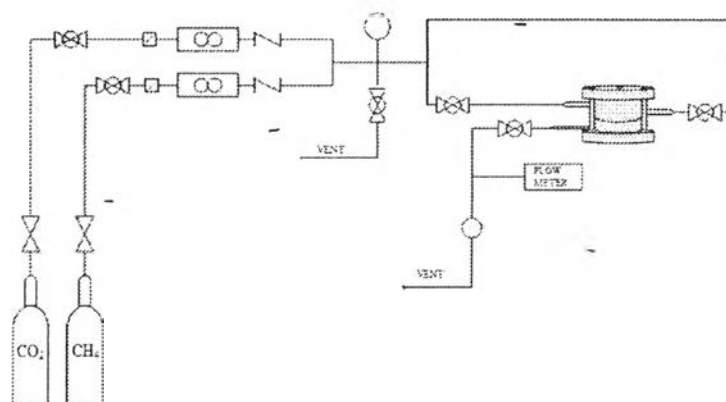
$$S_{A/B} = \frac{P_A}{P_B} \qquad (2)$$

Figure 4.1 A schematic diagram of gas separation unit.

4.4 Results and Discussion

4.4.1 Preparation of Porous PVA/CaCO₃ Hybrid Composite

The PVA/CaCO$_3$ composite material was prepared from high molecular weight polyvinyl alcohol (Mw= 108,000 g/mol) as a polymer matrix, calcium carbonate as filler and the crosslinking agent was boric acid via dispersion of filler in polymer matrix. The mixture was removed the water as a solvent by freeze-drying method to achieve the porous composite material.

The porous PVA/CaCO$_3$ hybrid composites after freeze-drying were observed which it was found that the 3% of PVA content in the water showed the highest collapse and shrinkage when compared with 5% and 7%. The collapse of samples caused by PVA concentration in water, the lower percentage of PVA in water gave a higher collapse and shrinkage of samples because it has more space area after removing of water from materials. Moreover, PVA, which has high molecular weight and flexible chain; the shrinkage was occurred by the surface force

between PVA and water after removal of solvent by sublimation method (Krokida, *et al.*, 1998 and Safranova, *et al.*, 2007). However, the higher viscosity of polymer solution may prevent or reduce the shrinkage meaning that the increase in PVA concentration led to a decrease in the collapse and shrinkage materials. Figure 4.2 were represented the destruction of the porous materials after using a freeze drying method with 3% and 5% PVA in water whereas 7% PVA content as a result from an increase of PVA content led to a decrease of the shrinkage of materials
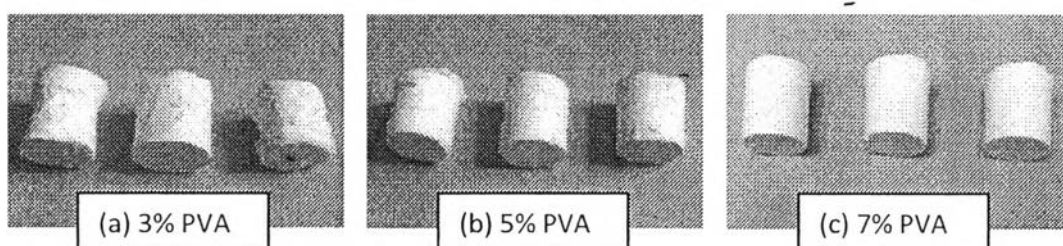

Figure 4.2 (a) 3% PVA, (b) 5% PVA and (c) 7% PVA after freeze-drying.

The morphological configurations of porous PVA/CaCO₃ hybrid composites were studied as shown 3-D interconnected porous structure or dendritic type structure by using high molecular weight PVA in Figure 4.3 from SEM images (Gawryla, *et al.*, 2009). The Figure 4.3 (a) shows 5% PVA with the weight ratio PVA: CaCO₃ of 1:1 and the Figure 4.3 (b) is 7% with the same weight ratio of polymer and filler.

It is seen that from the Figure 4.3.The structural appearance of porous materials after freeze-drying method were changed the pore wall thickness with increasing the PVA concentration from 5% to 7%. The increase of PVA concentration, the size of pore created by ice crystal was scaled down and the difficult of ice formation to form was increased (Gutierrez, *et al.*, 2007). Therefore, a higher concentration of PVA solution, a smaller of both ice crystal particles and macropores size which conclude the pore wall thickness of 7%PVA is greater than 5%PVA from SEM images (Lozinsky,*et al.*, 1998).
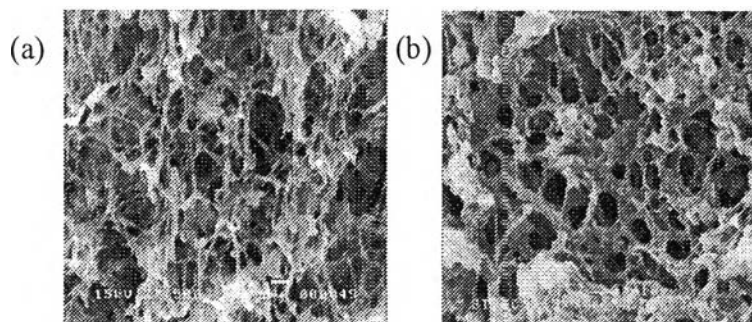
Figure 4.3 SEM images of (a) 5% PVA and (b) 7% PVA with the same weight ratio 1:1 (PVA: $CaCO_3$).

4.4.2 The Chemical Structure of PVA/CaCO$_3$ Composite

The FT-IR spectrum in the range of wave number 4000-400 cm^{-1} was characterized in order to show the specific chemical groups of raw materials, including polyvinyl alcohol used as a matrix of the hybrid porous composites, calcium carbonate act as filler and $PVA/CaCO_3$ composite are shown in Figure 4.4.

FT-IR spectra of pristine PVA is shown in Figure 4.4 (a), which are consist of the broaden absorption peak of predominant -OH stretching, asymmetric stretching of CH_2 and C=C stretching at 3433, 2940, 1653 cm^{-1} and at approximately 1095 and 1143 cm^{-1} for the C-O group. The weak adsorption at 918 cm^{-1} is assigned to C-C stretching vibration of PVA (Yang, *et al.*, 2004, Zheng, *et al.*, 2008 and Wang, *et al.*, 2010).In the Figure 4.4(c) FTIR spectra of the three peaks of calcium carbonate are illustrated at 713, 873, 1470cm^{-1} represented to $CaCO_3$ (Zheng, *et al.*, 2008). The FTIR spectra of PVA-$CaCO_3$ porous hybrid composite as shown in the Figure 4.4(b) represented peak similar as PVA spectra but the adsorption at 712, 874 and 1796 identify to calcium carbonate. The absorption from 1095 cm^{-1} of PVA in Figure 4.4(a) was shifted to 1100 cm^{-1}, describing the molecular interaction between organic and inorganic by using PVA and $CaCO_3$ (Zheng, *et al.*, 2008).
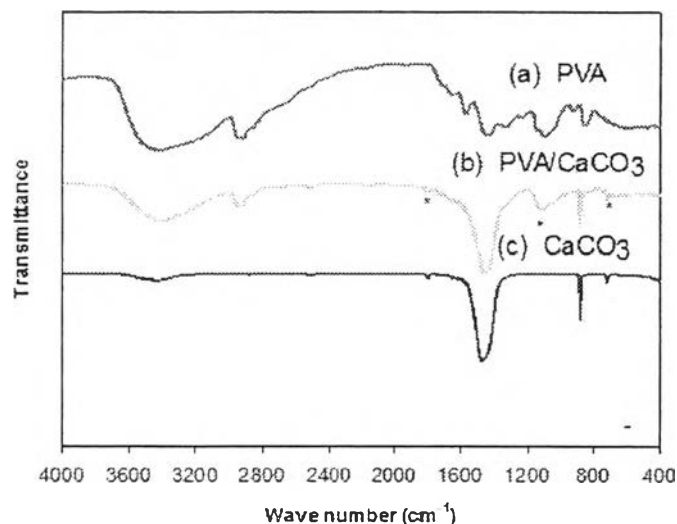
Figure 4.4 The FTIR spectra of (a), pure PVA, (b) porous PVA/CaCO₃ hybrid composite, (c) calcium carbonate (CaCO₃).

4.4.3 Thermal Behaviors of PVA/CACO₃ Composite

Thermogravimetric analyses (TGA) of PVA and PVA/CaCO₃ porous composite have been studied the decomposition of PVA had three steps degradation as shown in Figure4.5 (a) and 4.6(a). The first stage involves the dehydration of the water-absorbed or the volatile in material by decreasing about 10% weight loss (Xing, *et al.*, 2011).According to Gilman *et al.*, (1995) and Peng *et al.*, (2007),the second stage is related to elimination of hydroxyl groups from high-hydrolyzed PVA which are obtained the two types of polyene formations: conjugated and non-conjugated polyenes and low molecular weight product at the temperature between 240-345 °C, as shown in Figure 4.7 schemes(a). Besides, the degradation curve region of temperature 350-485 °C is corresponding to chain-scission reaction of the polyenes in order to break the polymer backbone.

For the PVA/CaCO₃ porous hybrid composite as shown in Figure 4.5 (b),(c) and (d) by increasing CaCO₃ content, respectively, the last transition state of degradation showed the transformation of CaCO₃ to CaO residue at the temperature between 560-748°C (Halikia, *et al.*, 2001). The percentage of weight loss were increased with CaCO₃ content increase compared to pure PVA 7%, there was no

weight loss at temperature above 500°C. On the other hand, the ratios of $CaCO_3$ content decrease with PVA content increase (Figure 4.6(b), (c) and (d)).
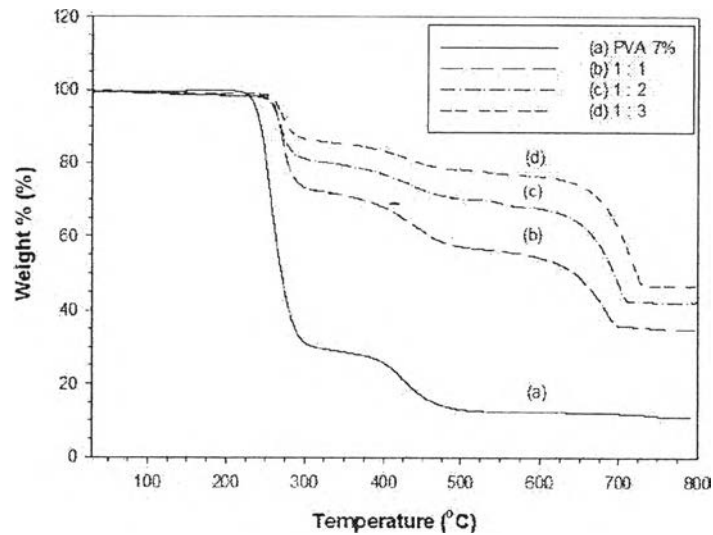

Figure 4.5 TGA thermograms of (a)7%PVA, (b) 7%PVA with weight ratio 1:1 (PVA:CaCO₃), (c)7%PVA (1:2), (d)7%PVA (1:3).
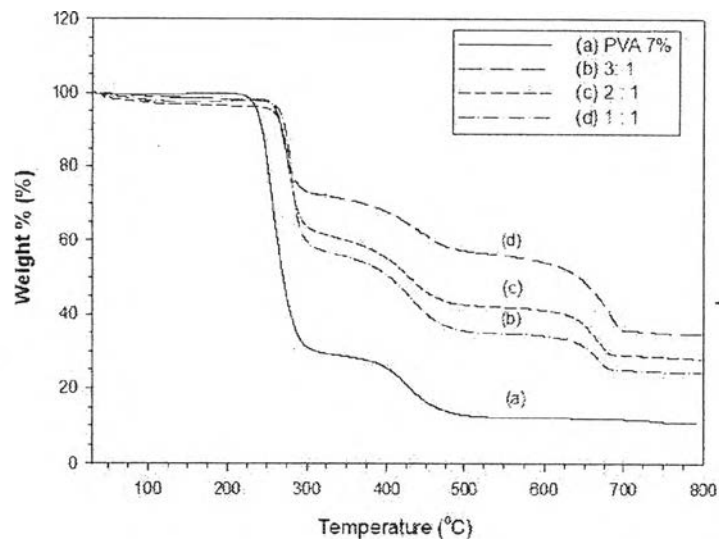

Figure 4.6 TGA thermograms of (a) 7%PVA, (b) 7%PVA with weight ratio 3:1 (PVA:CaCO₃), (c)7%PVA (2:1), (d)7%PVA (1:1).
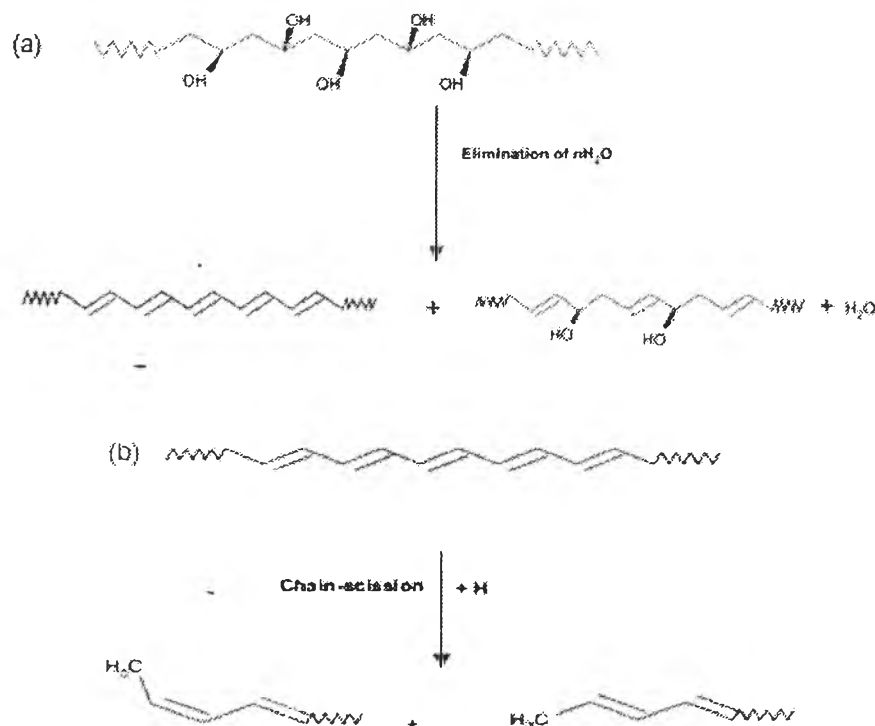
Figure 4.7 Schematic diagram of (a) Elimination reaction of hydroxyl group from PVA, (b) Chain scission reaction of polyenes (Gilman, *et al.*, (1995) and Peng, *et al.*, (2007)).

4.4.4 Morphology of PVA/CaCO₃ Porous Hybrid Composite

SEM images showed 7%PVA in water with increasing in PVA content of weight ratio and increasing in $CaCO_3$ content of weight ratio in Figure 4.8 and Figure 4.9, respectively. There are exhibit 3-D interconnected porous network. Figure 4.8 showed the addition of 1:1, 2:1 and 3:1 of PVA content in (PVA:CaCO₃) weight ratio illustrated that pore wall thickness have many small pore size (Fig. 4.8(d) and 4.8(f)). Due to PVA has high molecular weight and closely entanglement through hydrogen bonding which the small ice crystals formation during the freeze-drying method (Hou, *et al.*, 2013). Hence, the pore size is scale down and PVA matrix has a thicker pore wall.
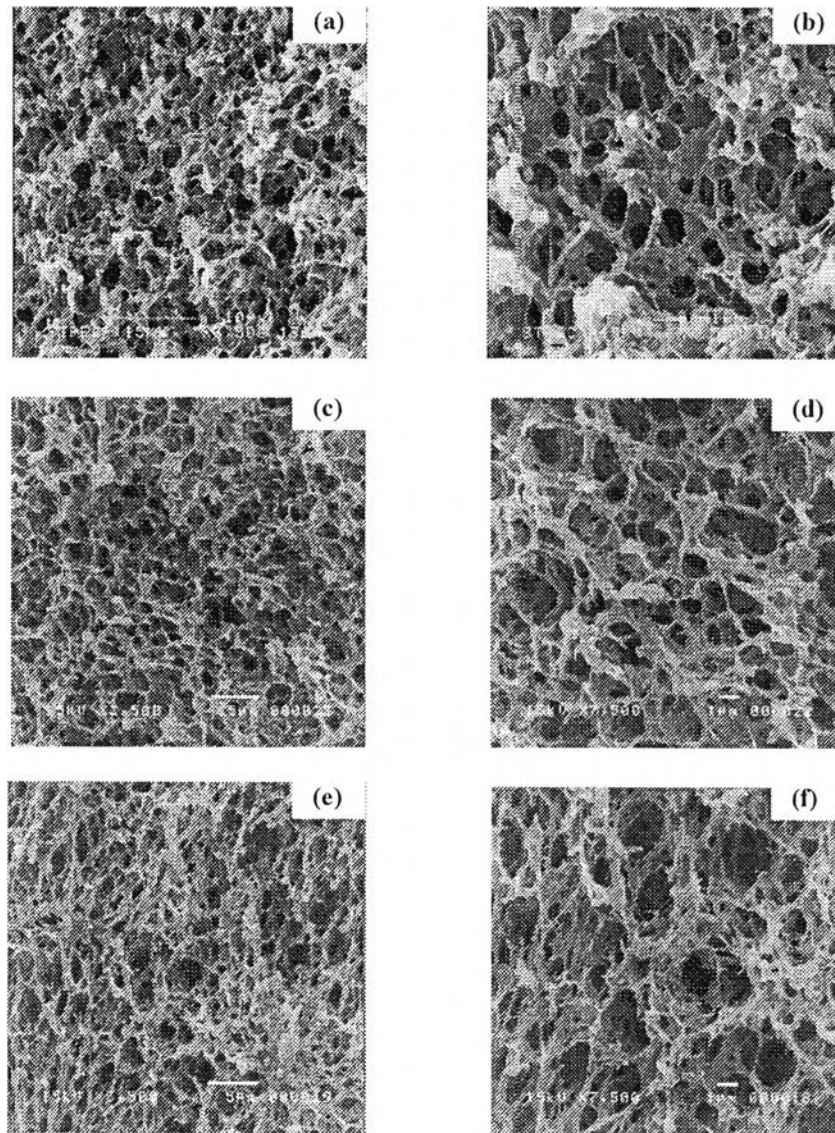
Figure 4.8 SEM images at different magnification (left= 3500 times, right= 7500 times) of 7%PVA in water with weight ratio of PVA: $CaCO_3$: (a, b) 7%PVA (1:1), (c, d) 7%PVA (2:1) and (e, f) 7%PVA (3:1).

In case of increasing in $CaCO_3$ contents as showed in Figure 4.9 (a,b)and (c,d) at the (PVA:$CaCO_3$) weight ratio 1:2 and 1:3, respectively. There has an agglomeration of $CaCO_3$due to large amount on PVA matrix so that porous hybrid composite with increasing of $CaCO_3$ led to a low dispersion in the matrix. Therefore, a higher $CaCO_3$ than PVA content in porous composite rarely have small

pore on the PVA matrix compared with a change in PVA content at the same magnification of 7500 times on the right (Figure 4.9 (b) and 4.9 (d).
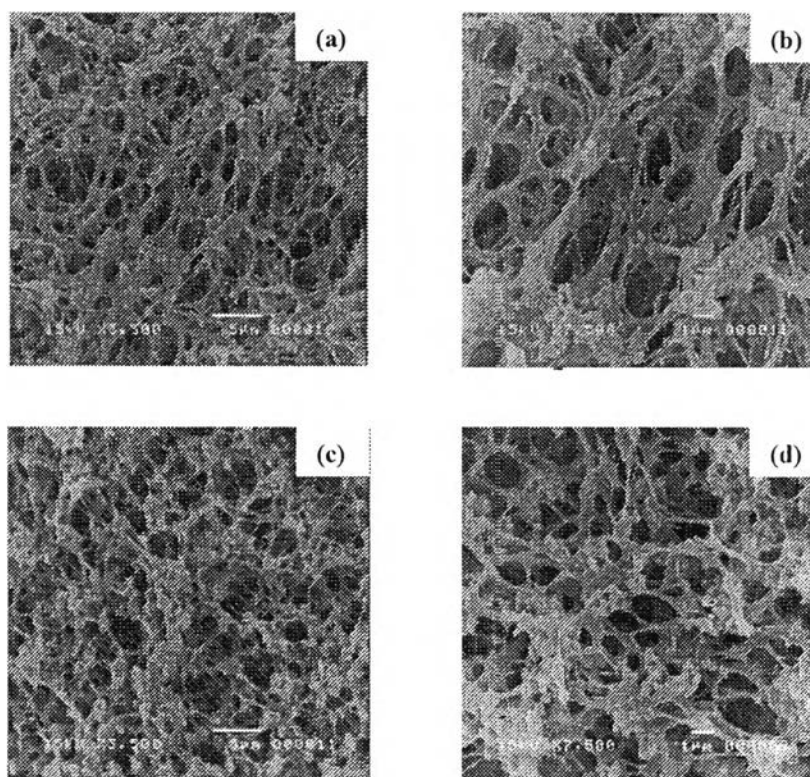

Figure 4.9 SEM images at different magnification (left=3500 times, right=7500 times) of 7%PVA in water with weight ratio of PVA: $CaCO_3$: (a, b) 7%PVA (1:2) and (c, d) 7%PVA (1:3).

4.4.5 Microstructure of Porous Hybrid Composite

The techniques for identifying the porous structure of porous hybrid composites were characterized from N_2 adsorption/desorption isotherm at 77 K in order to distinguish the different amount weight ratio of PVA: $CaCO_3$ influenced on overall surface area, total pore volume and average pore diameters with calculating from Brunauer-Emmett-Teller (BET) method as reviewed in the Table 4.1(Inagaki, 2009).

Porosity of porous materials was characterized by using helium-pycnometry. The gas pycnometry presents the true density and skeletal volume,

which porosity was calculated from the following equations (Parmentier, *et al.*, 2001).

$$Porosity = \frac{Bulk\ volume - Skeletal\ volume}{Bulk\ volume} \times 100 \qquad (Eq6.1)$$

$$Porosity = \left[1 - \left(\frac{skeletal\ volume}{Bulk\ volume}\right)\right] \times 100 \qquad (Eq6.2.)$$

Where bulk volume was calculated by their mass and volume from the equation $D = \frac{m}{V}$ (m= mass of sample, V = volume of sample) and bulk volume measurement by using vernier caliper to measure the materials. Skeletal volume was obtained from the true density of helium pycnometer with the same mass from bulk sample and then converted into the skeletal volume.

- *4.4.5.1 The effect of PVA content on the porous structure*

The surface area analysis of porous PVA/CaCO$_3$ hybrid composite was summarized in Table 4.1 which has the abbreviation of the sample, for example, 7%(1:1) meaning that 7% of PVA and the weight ratio PVA: CaCO$_3$ of 1:1. The effect of weight ratio between PVA: CaCO$_3$ was explained that the PVA content in the composite materials influenced on the porous structure, surface area and total pore volume. The results showed an increasing weight ratio of PVA led to change in the surface area and total pore volume due to higher concentration of polymer matrix induced thicker pore wall and smaller size of pores. The surface area increases from 15.61 to 54.97 m^2/g while total pore volume decrease from 55.26 nm to 41.82 nm. Therefore, 7% PVA (3:1) is the highest total surface area which is related to the highest total pore volume and higher porosity (Aravind, *et al.*,2011). The SEM photographs in Figure4.8(e, f) are supported the 7%PVA with 3:1 ratio are higher surface area and porosity due to increasing smaller pore size corresponding to increasing of PVA concentration (Nie, *et al.*, 2012, Li, *et al.*, 2001 and Fu, *et al.*, 2013).

Table 4.1 The summarization of surface analysis with increasing of PVA content

7%PVA with various ratios (PVA:CaCO₃)	Total surface area (m²/g)	Total pore volume (cc/g)	Average pore diameter (nm)	% Porosity (%)
7% (1:1)	14.55 ± 1.49	0.21 ± 0.01	54.37 ± 1.27	78.64
7% (2:1)	32.26 ± 3.20	0.41 ± 0.02	51.21 ± 7.95	80.43
7% (3:1)	52.55 ± 3.43	0.62 ± 0.06	47.40 ± 7.89	82.37

4.4.5.1 The effect of CaCO₃ content on the porous structure

However, the surface area analysis of increasing $CaCO_3$ content in weight ratio showed the results in Table 4.2. It can be seen that amount of $CaCO_3$ had slightly change in the surface area whereas average pore diameter was related to porosity by 7%(1:2) had high average pore diameter and lower porosity because of larger pore size as confirmed by SEM images in Figure 4.9(a-b) Therefore, an increasing of $CaCO_3$ might be slightly changed in surface area due to the random agglomeration in porous microstructure with low dispersion of $CaCO_3$ particles led to the roughness on the surface area.

Table 4.2 The summarization of surface analysis with increasing of $CaCO_3$ content

7%PVA with various ratios (PVA:CaCO₃)	Total surface area (m²/g)	Total pore volume (cc/g)	Average pore diameter (nm)	% Porosity (%)
7% (1:1)	14.55 ± 1.49	0.21 ± 0.01	54.37 ± 1.27	78.64
7% (1:2)	21.61 ± 1.85	0.36 ± 0.12	66.28 ± 27.76	73.89
7% (1:3)	18.77 ± 0.83	0.21 ± 0.03	45.9 ± 9.23	83.34

4.4.6 Gas Permeability

The permeation testing on $PVA/CaCO_3$ was tested in the single gas measurements. The permeation of these membranes was obtained in the sequence of CH_4 and CO_2 at room temperature and 10 psi after in steady state by let gas pass for 1 hour.

4.4.6.1 The effect of CO_2 and CH_4 the permeability on increasing PVA content

Figure 4.10 showed that the CO_2 and CH_4 permeabilities of 7% PVA (1:1), 7% PVA (2:1) and 7% PVA (3:1) depending on molecular kinetic diameter of gases. Comparing of CO_2 and CH_4 molecules, CO_2 is a longer and smaller molecule than CH_4 which is a more compact molecule with a slightly larger cross-section due to the molecular kinetic diameter of CO_2 and CH_4 are 3.3 Å and 3.8 Å, respectively. Even at the small different molecular kinetic diameter of CO_2 and CH_4 of gas molecules results in the large amount of the diffusion rate that can be penetrated through the 3-D interconnected porous membrane. Different size of molecules could be separated by this membrane due to the different time spent inside the membrane which excluded large molecules first whereas smaller molecules have free accessibility to elute after similar to the size exclusion chromatography technique as shown in Figure 4.11. Therefore, the permeability of CH_4 is faster than that of CO_2. The presence of PVA content as a matrix led to increase the small pore in matrix assisted the diffusion rate of CO_2 molecules to penetrate through membrane when increasing of PVA content from 1:1 to 3:1, the CO_2 permeability was raised due to the weight ratio of PVA content increase as results of many small pores on the matrix with large amount of contact area of gas can be penetrated and high porosity. However, the permeability of CH_4 is higher than that of CO_2 because of the materials have a physical interaction (dipole-quadrupole) of polar group of PVA matrix and CO_2 molecules (Yang, *et al.*, 2012 and Semsarzadeh, *et al.*, 2013).
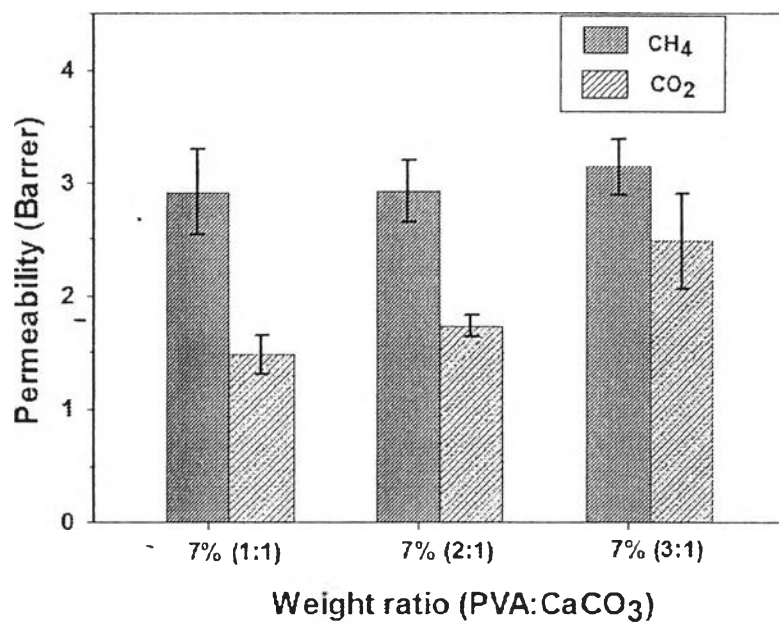
Figure 4.10 Permeability of CO_2 and CH_4 through 7%PVA with different PVA content.
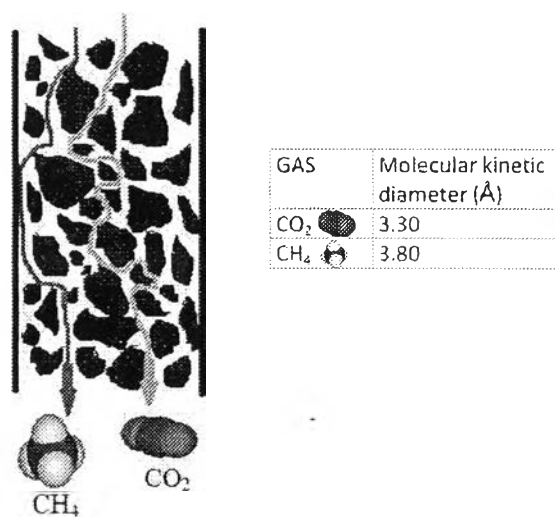

Figure 4.11 Complex pathway of gases molecules penetrate depending on their molecular kinetic diameter.

4.4.6.2 The effect of CO_2 and CH_4 the permeability on increasing CaCO₃ content

Figure 4.12 showed gas permeability of PVA/CaCO₃ with increasing of CaCO₃ content. The 3-D interconnected porous pathway is an effect on permeability depending on molecular kinetic diameter of gases similar to the gas permeability results of porous composite with increasing ratio of PVA as mentioned above. However, the permeability did not effect on the increasing of weight ratio of CaCO₃ due to a higher amount of CO_2 molecules on high porosity as confirmed by SEM (Fig. 4.9) and Table 4.2
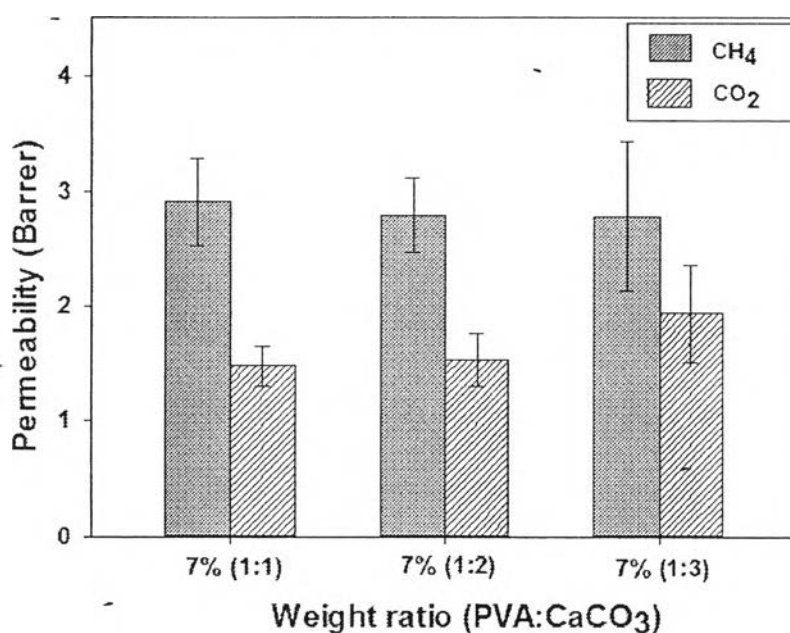

Figure 4.12 Permeability of CO_2 and CH_4 through 7%PVA with different CaCO₃ content.

4.4.6.3 The effect of different weight ratio (PVA:CaCO₃) on the CH_4/CO_2 selectivity

The CH_4/CO_2 selectivity for PVA/CaCO₃ membrane at different weight ratio between PVA and CaCO₃ are showed in Figure 4.14. It can be seen that the CH_4/CO_2 selectivity decreased due to increasing of both PVA and CaCO₃ content in the weight ratio with the high porosity and containing the continuous pathways for gas penetrated through the porous PVA/CaCO₃ composites

membrane. Thus, the addition of the weight ratio provided higher chance for allowing of the gas molecule to diffuse throughout membrane.
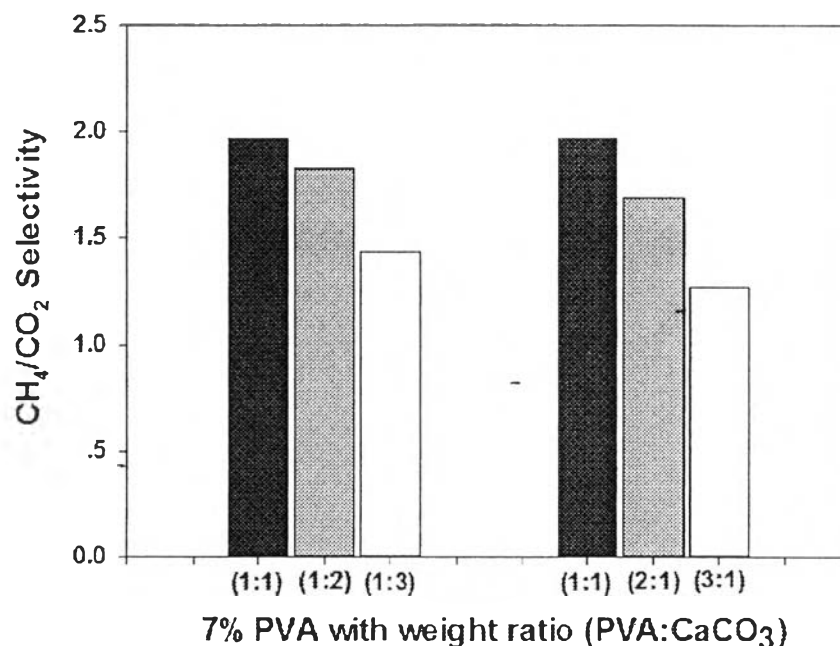

Figure 4.13 Effect of different weight ratio of PVA and $CaCO_3$ on CH_4/CO_2 selectivity

4.5 Conclusions

The synthesized of $PVA/CaCO_3$ green porous hybrid composite were successfully prepared from non-toxic raw materials, having lower shrinkage on 7% PVA concentration in water. The different weight ratio between PVA and $CaCO_3$ had effect on morphology and microstructure by increasing in weight ratio PVA content led to increasing the small pore size and surface area. The gas permeation was controlled by molecular kinetic diameter of penetrant gas through the 3-D interconnected complex pathway. Moreover, CO_2 molecules have the ability to interact with the polar group of polymer so that the penetrance of CH_4 is faster than CO_2. The optimum ratio of 7% PVA in the water was 1:1 due to show a high CH_4/CO_2 selectivity compared to the ratio of increasing the both PVA and $CaCO_3$

showed high porosity with a result on high CO_2 permeability led to had low CH_4/CO_2 selectivity.

4.6 Acknowledgements

4.7 References

Abedini, R. and Nezhadmoghadam, A. (2010). Application of Membrane in Gas Separation Processes: Its Suitability and Mechanisms. Petroleum & Coal 52(2), 69-80.

Ali, M., Kahder, M.M. and Al-Saad, K.A. (2012). Properties of nanoclay-PVA composite materials. Qatar Foundation Annual Research Forum Proceedings(2012), EEP2.

Aravind, P.R. and Soraru, G.D. (2011). Porous silicon oxycarbide glasses from hybrid ambigels. Microporous and Mesoporous Materials 142(2–3), 511-517.

Fu, Y.-C., Chen, C.-H., Wang, C.-Z., Wang, Y.-H., Chang, J.-K., Wang, G.-J., Ho, M.-L.and Wang, C.-K. (2013). Preparation of porous bioceramics using reverse thermo-responsive hydrogels in combination with rhBMP-2 carriers: In vitro and in vivo evaluation. Journal of the MechanicalBehavior of Biomedical Materials 27(0), 64-76.

Gawryla, M.D. and Schiraldi, D.A. (2009). Novel Absorbent Materials Created via Ice Templating. Macromolecular Materials and Engineering 294(9), 570-574.

Gilman, J. W., VanderHart, D. L., and Kashiwagi, T. (1995). Chapter. 11. Thermal Decomposition. Chemistry of Poly(vinyl alcohol) char Characterization and Reactions with Bismaleimides. ACS Symposium Series 599; American Chemical Society. Fire and Polymers II: Materials

and Tests for Hazard Prevention. National Meeting. 208th. American Chemical Society. Washington. DC. Nelson. G. L.. Editor(s). 161-185.

Gutiérrez, M.C., García-Carvajal, Z.Y., Jobbágy, M., Rubio, F., Yuste, L., Rojo, F., Ferrer, M.L. and del Monte, F. (2007). Poly(vinyl alcohol) Scaffolds with Tailored Morphologies for Drug Delivery and Controlled Release. Advanced Functional Materials 17(17), 3505-3513.

Halikia, I., Zoumpoulakis, L., Christodoulou, E. and Prattis, D. (2001). Kinetic study of the thermal decomposition of calcium carbonate by isothermal methods of analysis. European Journal of Mineral Processing and Environmental Protection 1(2), 89-102.

Hou, R., Zhang, G., Du, G., Zhan, D., Cong, Y., Cheng, Y. and Fu, J. (2013). Magneticnanohydroxyapatite/PVA composite hydrogels for promoted osteoblast adhesion and proliferation. Colloids and Surfaces B: Biointerfaces 103(0), 318-325.

Inagaki, M. (2009). Pores in carbon materials-importance of their control. New Carbon Materials 24(3). 193-232.

Krokida, M.K., Karathanos, V.T. and Maroulis, Z.B. (1998). Effect of freeze-drying conditions on shrinkage and porosity of dehydrated agricultural products. Journal of Food Engineering 35(4), 369-380.

Kickelbick, G. (2007). Hybrid materials: Wiley-vch., 1-10.

Houmard, M., Vasconcelos, D.C.L., Vasconcelos, W.L., Berthomé, G., Joud, J.C. and Langlet, M. (2009). Water and oil wettability of hybrid organic–inorganic titanate–silicate thin films deposited via a sol–gel route. Surface Science 603(17), 2698-2707.

Li, M., Minoura, N., Dai, L. and Zhang, L. (2001). Preparation of Porous Poly(vinyl alcohol)-Silk Fibroin (PVA/SF) Blend Membranes. Macromolecular Materials and Engineering 286(9), 529-533.

Li, S., Carreon, M.A., Zhang, Y., Funke, H.H., Noble, R.D. and Falconer, J.L. (2010). Scale-up of SAPO-34 membranes for CO2/CH4 separation. Journal of Membrane Science 352(1–2), 7-13.

Lozinsky, V.I. and Plieva, F.M. (1998). Poly(vinyl alcohol) cryogels employed as matrices for cell immobilization. 3. Overview of recent research and developments. Enzyme and Microbial Technology 23(3–4), 227-242.

Nie, L., Chen, D., Suo, J., Zou, P., Feng, S., Yang, Q., Yang, S. and Ye, S. (2012).

Physicochemical characterization and biocompatibility in vitro of biphasic calcium phosphate/polyvinyl alcohol scaffolds prepared by freeze-drying method for bone tissue engineering applications.Colloids and Surfaces B: Biointerfaces100(0), 169-176.

Parmentier, J., Soraru, G.D., and Babonneau, F., (2001). Influence of the microstructure on the high temperature behavior of gel-derived SiOC glasses, Journal of the European Ceramic Society, 21, 817-824

Peng, Z. and Kong, L.X. (2007). A thermal degradation mechanism of polyvinyl alcohol/silica nanocomposites. Polymer Degradation and Stability 92(6), 1061-1071.

Safronova, T. V., Shekhirev, M. A., and Putlyaev, V. I. (2007). Ceramics based on calcium hydroxyapatite synthesized in the presence of polyvinyl alcohol. Glass and Ceramics, 64, 32 – 36.

Semsarzadeh, M.A. and Ghalei, B. (2013). Preparation, characterization and gas permeation properties of polyurethane–silica/polyvinyl alcohol mixed matrix membranes. Journal of Membrane Science 432(0), 115-125.

Sridhar, S., Smitha,B., and Aminabhavi,T.M. (2007) Separation of carbon dioxide from natural gas mixtures through polymeric membranes—a-review, Sep. Purif. Rev. 36 113–174.

Wang, C., Piao, C., Zhai, X., Hickman, F.N. and Li, J. (2010). Synthesis and character of super-hydrophobic CaCO3 powder in situ. Powder Technology 200(1–2), 84-86.

Xing, R. and Ho, W.S.W. (2011). Crosslinked polyvinyl alcohol–polysiloxane/fumed silica mixed matrix membranes containing amines for CO2/H2 separation. Journal of Membrane Science 367(1–2), 91-102.

Yang, J.M., Su, W.Y., Leu, T.L. and Yang, M.C. (2004). Evaluation of chitosan/PVA blended hydrogel membranes. Journal of Membrane Science 236(1–2), 39-51.

Yang, S., Sun, J., Ramirez-Cuesta, Anibal J.C., Samantha K., William I. F.D., Anderson P. D., Newby R., Blake J. A., Parker J. E., Chiu C. T., Schroder M. (2012). Selectivity and direct visualization of carbon dioxide and sulfur dioxide in a decorated porous host. Nature Chemistry 4(11), 887-894.

Zhang, W. (2010). Experimental Investigation on Gas Separation Using Porous Membranes: Universitätsbibliothek.

Zheng, G.Q., Li, X.D., Wang, X.M., Ma, J.F. and Gu, Z.W. (2008). Structural characteristics of poly(vinyl alcohol)&calcium carbonate composites prepared by sequential method. Advances in Applied Ceramics 107(1), 46-51.